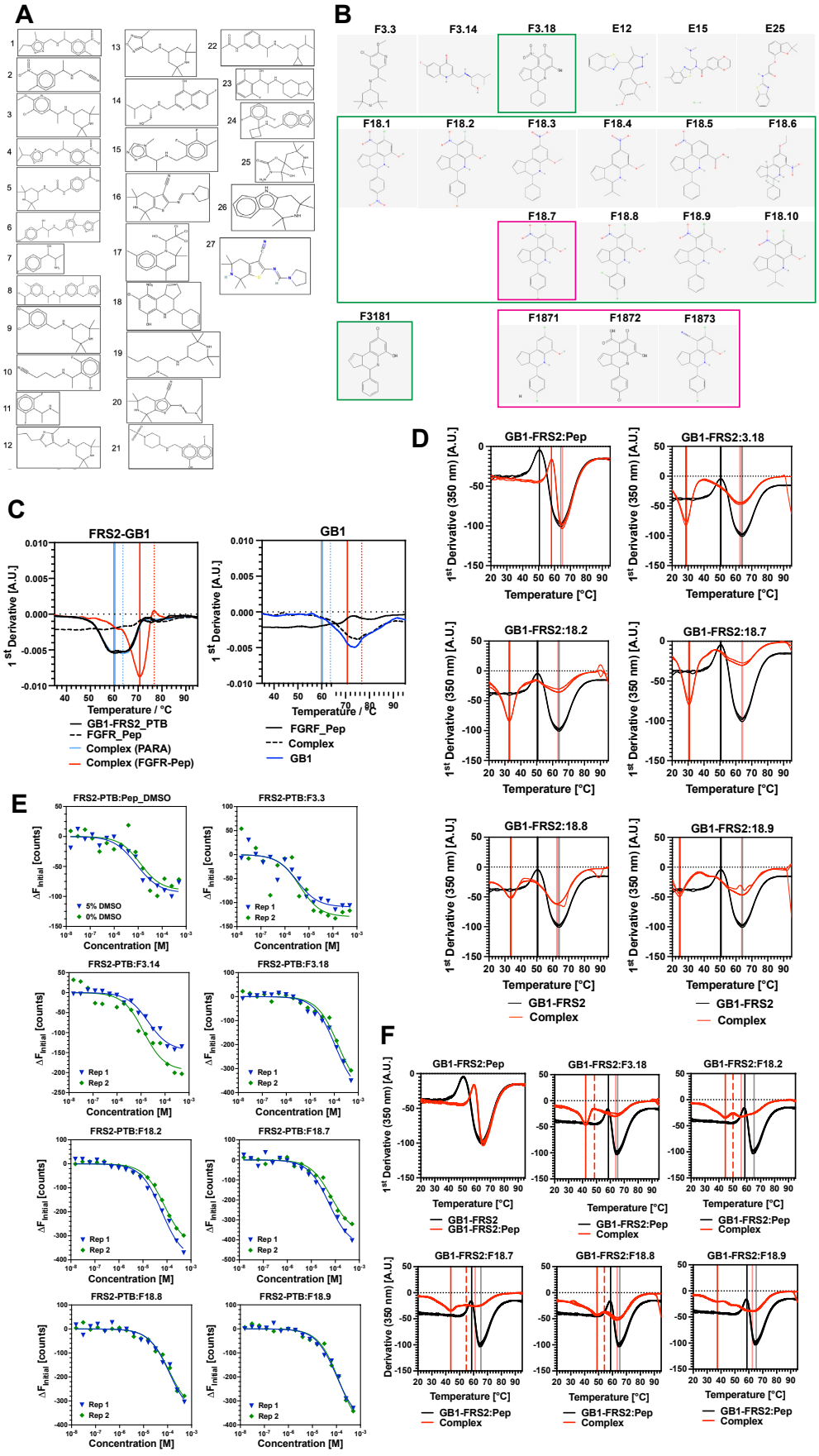
A
B
F3.3
F3.14
F3.18
E12
E15
E25
F18.1
F18.2
F18.3
F18.4
F18.5
F18.6
F18.7
F18.8
F18.9
F18.10
F3181
F1871
F1872
F1873
C
FRS2-GB1
GB1
1st Derivative [A.U.]
Temperature / °C
GB1-FRS2_PTB
FGFR_Pep
Complex (PARA)
Complex (FGFR-Pep)
FGRF_Pep
Complex
GB1
D
GB1-FRS2:Pep
GB1-FRS2:3.18
GB1-FRS2:18.2
GB1-FRS2:18.7
GB1-FRS2:18.8
GB1-FRS2:18.9
1st Derivative (350 nm) [A.U.]
Temperature [°C]
GB1-FRS2
Complex
E
FRS2-PTB:Pep_DMSO
FRS2-PTB:F3.3
FRS2-PTB:F3.14
FRS2-PTB:F3.18
FRS2-PTB:F18.2
FRS2-PTB:F18.7
FRS2-PTB:F18.8
FRS2-PTB:F18.9
ΔFinitial [counts]
Concentration [M]
5% DMSO
0% DMSO
Rep 1
Rep 2
F
GB1-FRS2:Pep
GB1-FRS2:F3.18
GB1-FRS2:F18.2
GB1-FRS2:F18.7
GB1-FRS2:F18.8
GB1-FRS2:F18.9
1st Derivative (350 nm) [A.U.]
Derivative (350 nm) [A.U.]
Temperature [°C]
GB1-FRS2
GB1-FRS2:Pep
Complex

Figure S1

A) Structures of selected F3 series compounds. **B)** Structures of compounds used in the study. Green box: F3.18 and analogs, magenta box: F18.7 biosteres. **C)** Plotted first derivatives of nanoDSF analysis of GB1-FRS2_PTB or GB1 alone or in combination with FGFR_PEP across temperature gradient recorded at 350 nm. **D)** Plotted first derivatives of nanoDSF analysis of GB1-FRS2_PTB or GB1 in the presence of F3.18 and structural analogs of F3.18 recorded at 350 nm. **E)** MST analysis by initial fluorescence change of shortlisted F3 series compounds. **F)** Competition assays of compounds against FGFR_PEP. Plotted first derivatives of nanoDSF analysis recorded at 350 nm of GB1-FRS2_PTB are shown. Black: GB1-FRS2_PTB:FGFR_PEP, Red: GB1-FRS2_PTB:FGFR_PEP plus added compound.

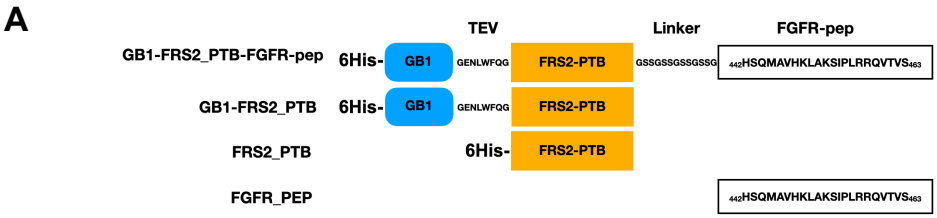
A
TEV
Linker
FGFR-pep
GB1-FRS2_PTB-FGFR-pep
6His-
GB1
GENLWFQG
FRS2-PTB
GSSGSSGSSGSSG
442HSQMAVHKLAKSIPLRRQVTVS463
GB1-FRS2_PTB
6His-
GB1
GENLWFQG
FRS2-PTB
FRS2_PTB
6His-
FRS2-PTB
FGFR_PEP
442HSQMAVHKLAKSIPLRRQVTVS463

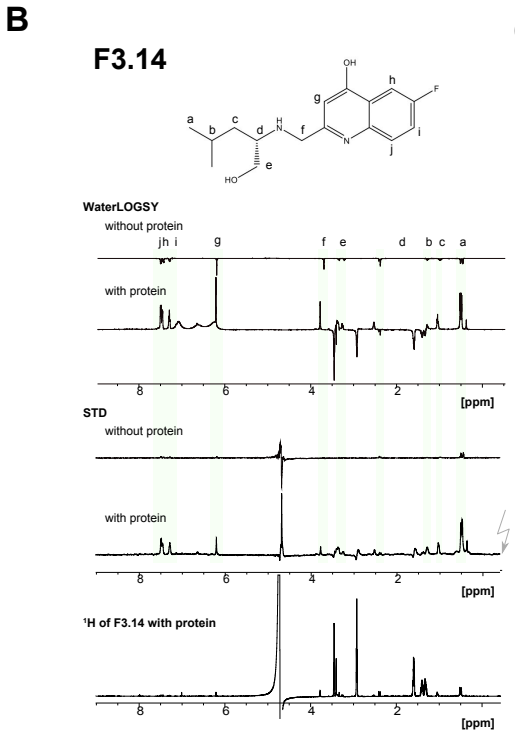
B
F3.14
WaterLOGSY
without protein
with protein
[ppm]
STD
without protein
with protein
[ppm]
¹H of F3.14 with protein
[ppm]

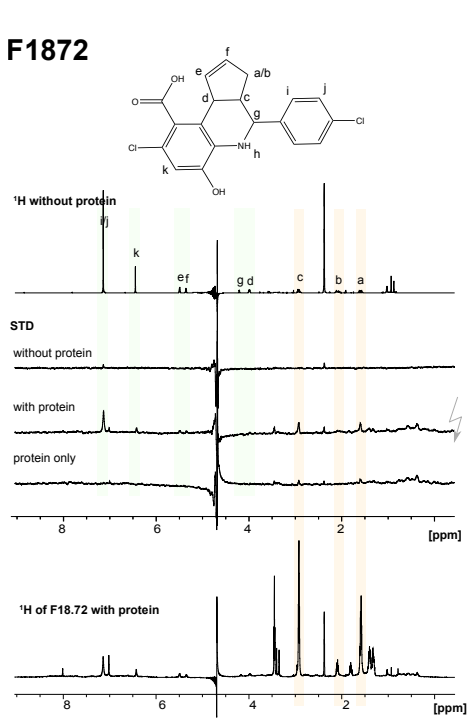
C
F1872
¹H without protein
STD
without protein
with protein
protein only
[ppm]
¹H of F18.72 with protein
[ppm]

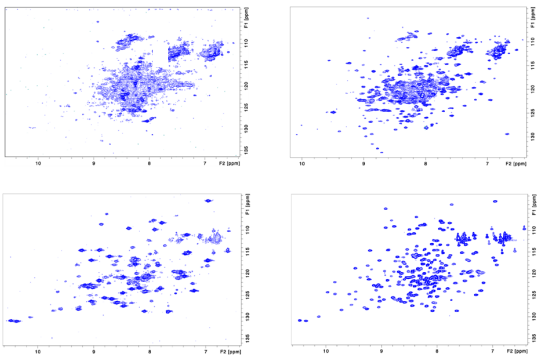
D

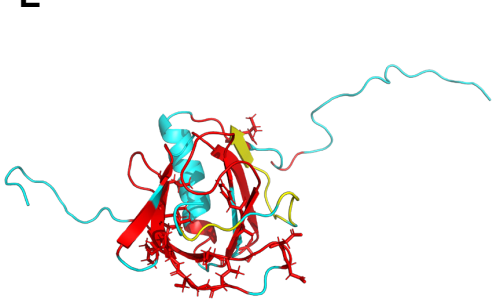
E

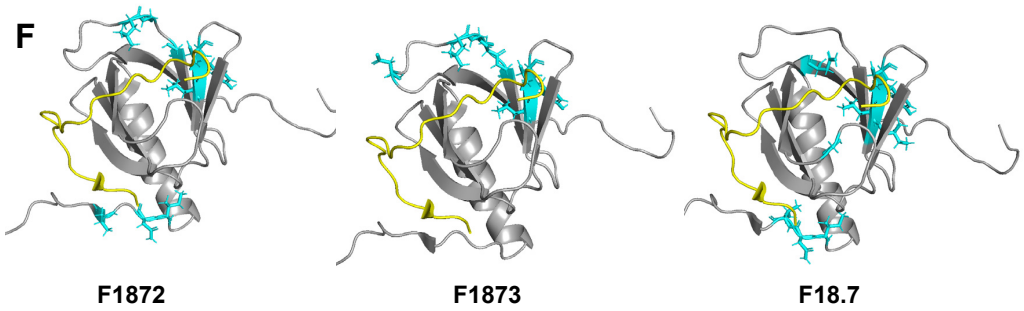
F
F1872
F1873
F18.7

Figure S2.

A) Structure of FRS2-PTB proteins expressed in *E.coli* and used in this study. Screening data for F3.14 **B**) and F1872 **C)**. Reference, STD and WATERLOGSY spectra are depicted. **D)** [^{15}N,^{1}H]-HSQC spectra of various FRS2 constructs. All spectra were recorded at 600 MHz , 25 ºC. **i** FRS2_PTB. **ii** FRS2_PTB + 2 equiv. FGRF1:PEP in 20 mM CHAPS. **iii** GB1-FRS2_PTB. **iv** GB1-FRS2_PTB-FGRF1_PEP. **E)** Assignment status. Residues for which backbone assignments were made are color-coded in red (protein) or yellow (FGFR1) on the structure of the non-covalent complex (pdb entry 1XR0). Assigned protein and peptide linker residues are depicted in red and yellow, respectively. Residues experiencing larger CSPs are depicted by sticks. F) Comparison of the CSPs observed upon interaction with F1872, F1873 and F18.7. FRS2-PTB residues are in grey, FGFR1_PEP in yellow. Residues experiencing larger CSPs are depicted by sticks in cyan.

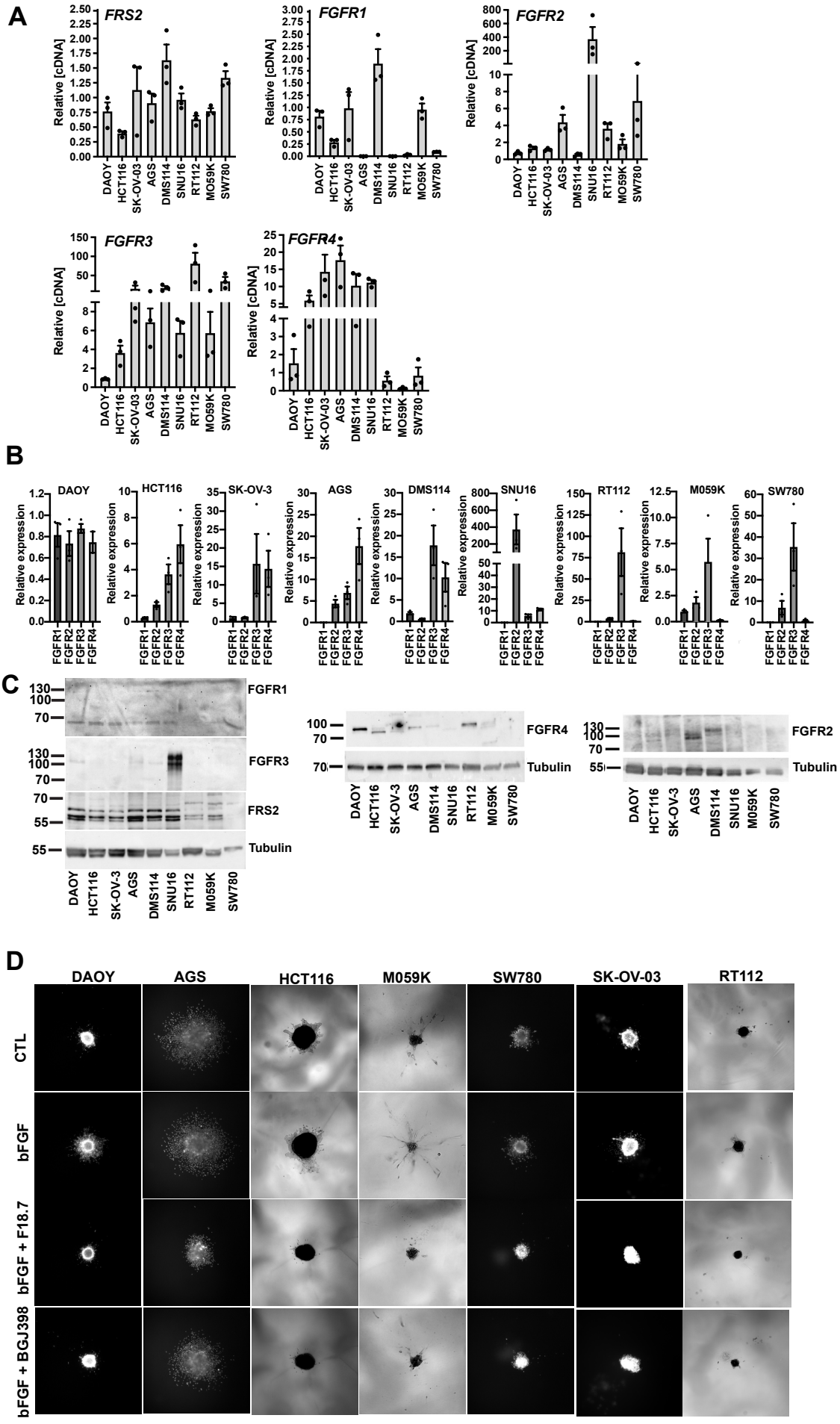
A
FRS2
FGFR1
FGFR2
FGFR3
FGFR4
Relative [cDNA]
DAOY
HCT116
SK-OV-03
AGS
DMS114
SNU16
RT112
MO59K
SW780
B
DAOY
HCT116
SK-OV-3
AGS
DMS114
SNU16
RT112
M059K
SW780
Relative expression
FGFR1
FGFR2
FGFR3
FGFR4
C
FGFR1
FGFR3
FRS2
Tubulin
FGFR4
FGFR2
D
DAOY
AGS
HCT116
M059K
SW780
SK-OV-03
RT112
CTL
bFGF
bFGF + F18.7
bFGF + BGJ398

Figure S3

A) RT-qPCR analysis of *FRS2* and *FGFR* expression across cancer cell lines used. Mean and SEM of n = 3 biological replicas is shown. **B)** Comparative RT-qPCR analysis of *FGFR* expression by cell line. Mean and SEM of n = 3 biological replicas is shown. **C)** IB analysis of FRS2 and FGFR expression across cell lines. **D)** Representative images of SIA of cell lines with indicated treatments at assay end-point.

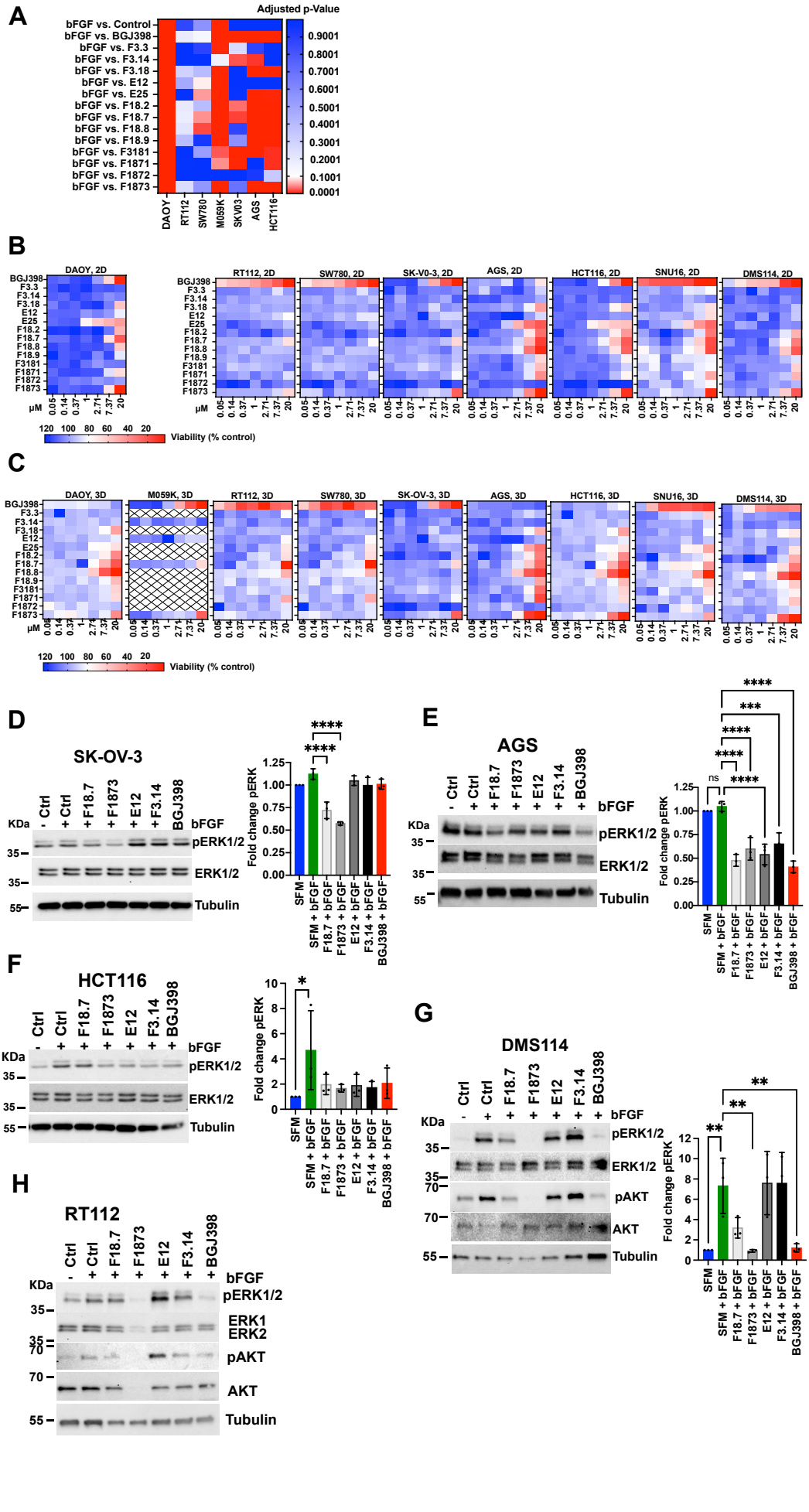
A
Adjusted p-Value
bFGF vs. Control
bFGF vs. BGJ398
bFGF vs. F3.3
bFGF vs. F3.14
bFGF vs. F3.18
bFGF vs. E12
bFGF vs. E25
bFGF vs. F18.2
bFGF vs. F18.7
bFGF vs. F18.8
bFGF vs. F18.9
bFGF vs. F3181
bFGF vs. F1871
bFGF vs. F1872
bFGF vs. F1873
DAOY
RT112
SW780
M059K
SKV03
AGS
HCT116
0.9001
0.8001
0.7001
0.6001
0.5001
0.4001
0.3001
0.2001
0.1001
0.0001
B
DAOY, 2D
RT112, 2D
SW780, 2D
SK-V0-3, 2D
AGS, 2D
HCT116, 2D
SNU16, 2D
DMS114, 2D
BGJ398
F3.3
F3.14
F3.18
E12
E25
F18.2
F18.7
F18.8
F18.9
F3181
F1871
F1872
F1873
µM
0.05
0.14
0.37
1
2.71
7.37
20
120 100 80 60 40 20
Viability (% control)
C
DAOY, 3D
M059K, 3D
RT112, 3D
SW780, 3D
SK-OV-3, 3D
AGS, 3D
HCT116, 3D
SNU16, 3D
DMS114, 3D
Viability (% control)
D
SK-OV-3
KDa
- Ctrl
+ Ctrl
+ F18.7
+ F1873
+ E12
+ F3.14
+ BGJ398
bFGF
pERK1/2
ERK1/2
Tubulin
35
55
Fold change pERK
****
SFM
SFM + bFGF
F18.7 + bFGF
F1873 + bFGF
E12 + bFGF
F3.14 + bFGF
BGJ398 + bFGF
E
AGS
ns
***
F
HCT116
*
G
DMS114
pAKT
AKT
**
H
RT112
ERK1
ERK2

Figure S4

A) Heat map of adjusted p-values of SIA analysis shown in Fig. 4A). **B)** Heat maps of cellTiter-Glo assays of cancer cell lines grown in 2D cultures depicting viability as % luminescence of control. **C)** Heat maps of 3D cellTiter-Glo assays of cancer cell lines grown in 3D cultures depicting viability as % luminescence of control. **D)** IB analysis of ERK phosphorylation in compound treated SK-OV-3 cells stimulated with bFGF. **E)** IB analysis of ERK phosphorylation in compound treated AGS cells stimulated with bFGF. **F)** IB analysis of ERK phosphorylation in compound treated HCT116 cells stimulated with bFGF. **G)** IB analysis of ERK and AKT phosphorylation in compound treated DMS114 cells stimulated with bFGF. **H)** IB analysis of ERK phosphorylation in compound treated RT112 cells stimulated with bFGF. Bar diagrams in D-H depict quantification of phosphorylation relative to unstimulated control. Mean fold change of phosphorylation of n = 3 independent experiments, SD and one-way ANOVA adjusted p-values of comparison to SFM+bFGF are shown.

A

Compound	10 mg/kg, PO	t1/2 (h)	Tmax (h)	Cmax (ng/ml)	AUClast (H*ng/ml)	AUCInf (h*ng/ml)	AUC/D (h*kg*ng/mL/mg)	AUC Extr (%)	MRT (h)	F (%)
F18.7	X	3.83	0.5	1395	3333	4069	407	18.1	4.71	85
F3.14	N/A									
E12	X	2.71	0.17	13	22	26	3	14.8	3.88	3

Compound	1 mg/kg, IV	t1/2 (h)	C0 (ng/ml)	AUClast (h*ng/ml)	AUCInf (h*ng/ml)	AUC Extr (%)	MRT (h)	Vss (L/kg)	CL (ml/min/kg)
F18.7	X	1.14	2873	393	398	1.2	0.29	0.7	42
F3.14	X	1.55	2703	410	413	0.5	0.52	1.3	40
E12	X	0.15	762	85	86	0.5	0.11	1.3	195

B

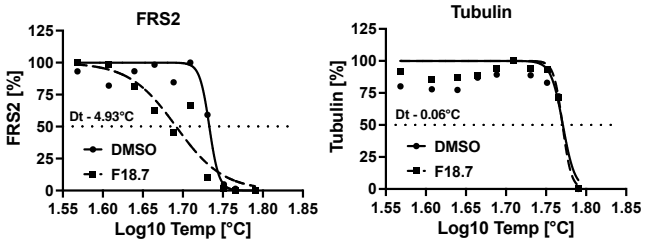

C

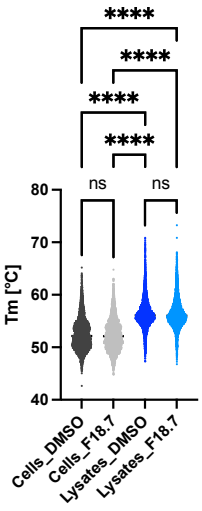

D

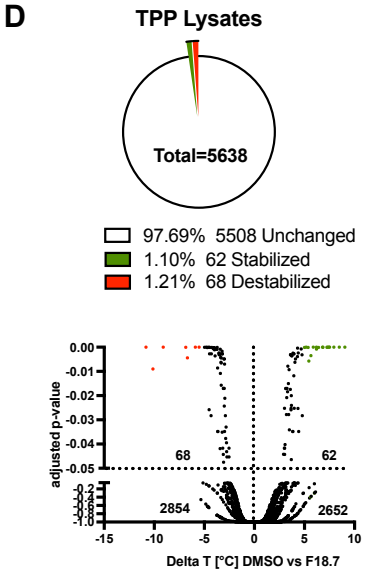

E

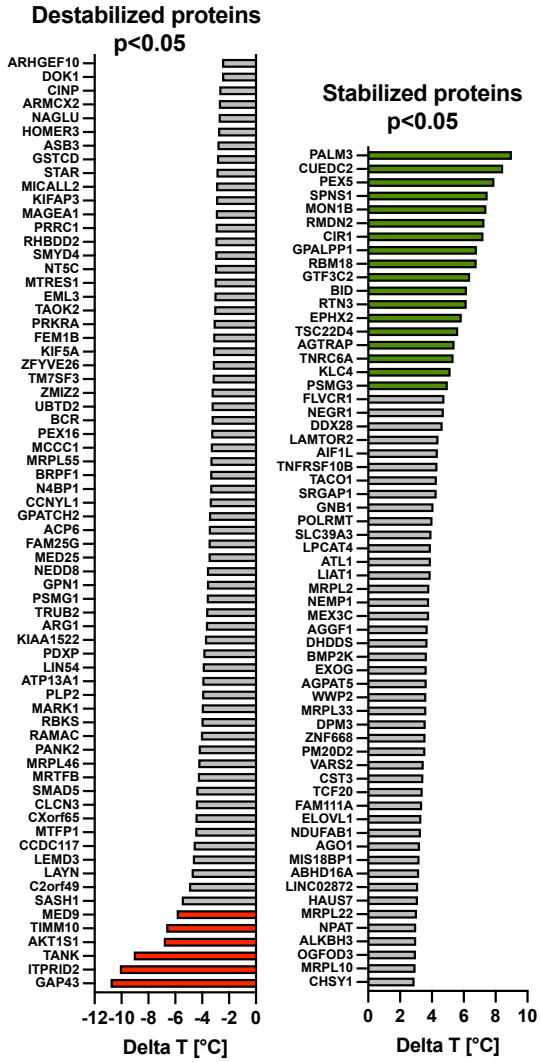

Figure S5

A) Summary of *in vivo* tolerability and PK analyses for F3.3, F3.14 and F18.7. **B)** Melting curves of FRS2 and tubulin in CETSA of DAOY lysates treated with either DMSO or F18.7. **C)** Comparison of measured T_m for detected proteins in TPP run of intact DAOY cells and DAOY lysates. **D)** Upper: Pie chart of percentage stabilized and destabilized proteins ($p<0.05$) from whole cell TPP from lysates analyzed in B. Lower: Volcano plot of ΔT_m from proteins of which high quality melting curves were obtained in both conditions. Red dots $\Delta T_m \geq -5°C$, green dots: $\Delta T_m \geq 5°C$. **E)** Scatterplot of all proteins with high quality melting curves in both conditions and bar plot with gene ID of proteins with altered T_m ($p<0.05$). Red bars $\Delta T_m \geq -5°C$, green bars: $\Delta T_m \geq +5°C$.

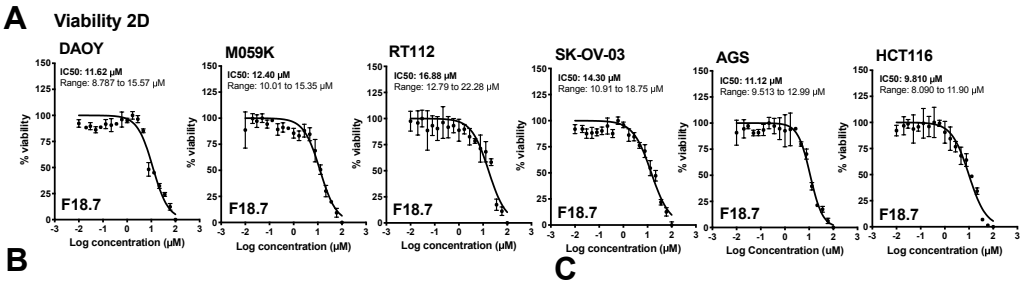
A
Viability 2D
DAOY
IC50: 11.62 µM
Range: 8.787 to 15.57 µM
M059K
IC50: 12.40 µM
Range: 10.01 to 15.35 µM
RT112
IC50: 16.88 µM
Range: 12.79 to 22.28 µM
SK-OV-03
IC50: 14.30 µM
Range: 10.91 to 18.75 µM
AGS
IC50: 11.12 µM
Range: 9.513 to 12.99 µM
HCT116
IC50: 9.810 µM
Range: 8.090 to 11.90 µM
% viability
F18.7
Log concentration (µM)
Log Concentration (uM)

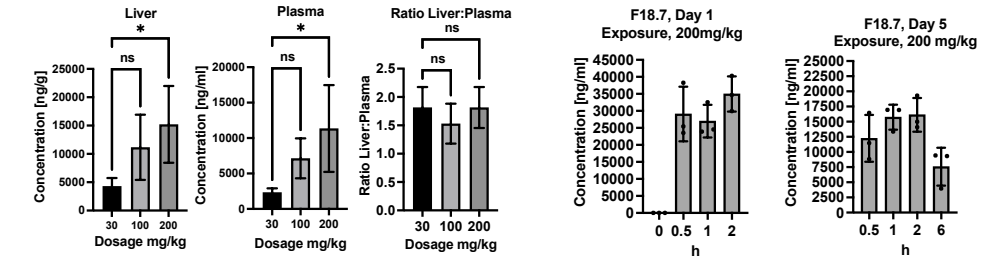
B
Liver
Plasma
Ratio Liver:Plasma
Concentration [ng/g]
Concentration [ng/ml]
Ratio Liver:Plasma
ns
*
Dosage mg/kg
C
F18.7, Day 1
Exposure, 200mg/kg
F18.7, Day 5
Exposure, 200 mg/kg
h

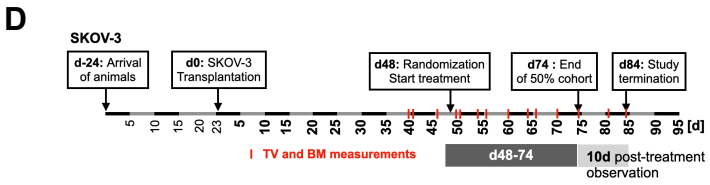
D
SKOV-3
d-24: Arrival of animals
d0: SKOV-3 Transplantation
d48: Randomization Start treatment
d74 : End of 50% cohort
d84: Study termination
[d]
TV and BM measurements
d48-74
10d post-treatment observation

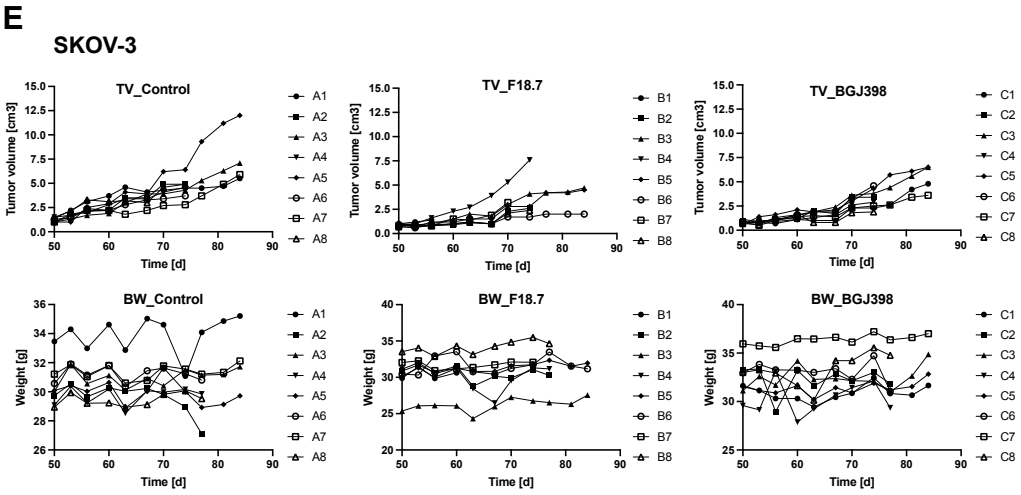
E
SKOV-3
TV_Control
TV_F18.7
TV_BGJ398
BW_Control
BW_F18.7
BW_BGJ398
Tumor volume [cm3]
Weight [g]
Time [d]

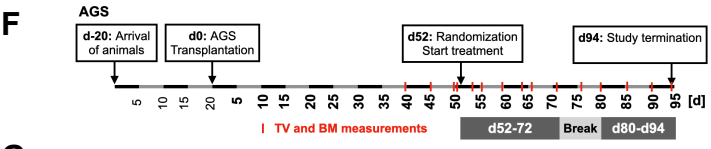
F
AGS
d-20: Arrival of animals
d0: AGS Transplantation
d52: Randomization Start treatment
d94: Study termination
[d]
TV and BM measurements
d52-72
Break
d80-d94

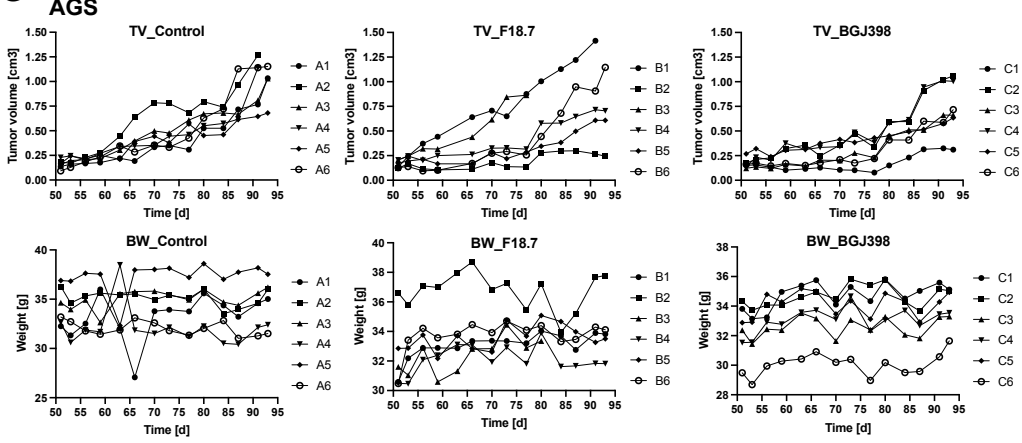
G
AGS
TV_Control
TV_F18.7
TV_BGJ398
BW_Control
BW_F18.7
BW_BGJ398
Tumor volume [cm3]
Weight [g]
Time [d]

Figure S6

A) IC_{50} curves of viability of cancer cell lines determined by CellTiterGlo assay after treatment with increasing concentrations of F18.7 in 2D cell viability assay. **B)** Exposure of F18.7 in plasma and liver 0.5 h after PO gavage of F18.7. **C)** Plasma exposure levels during 5x q.d. PO gavage of 200 mg/kg F18.7 at indicated times after gavage. **D)** Timeline and treatment scheme in SK-OV-3 mouse flank model. **E)** Tumor volume (TV) and body weight (BW) measurements in 6 mice per condition in SK-OV-3 model. **F)** Timeline and treatment scheme in AGS mouse flank model. **G)** Tumor volume (TV) and body weight (BW) measurements in 6 mice per condition in AGS model.

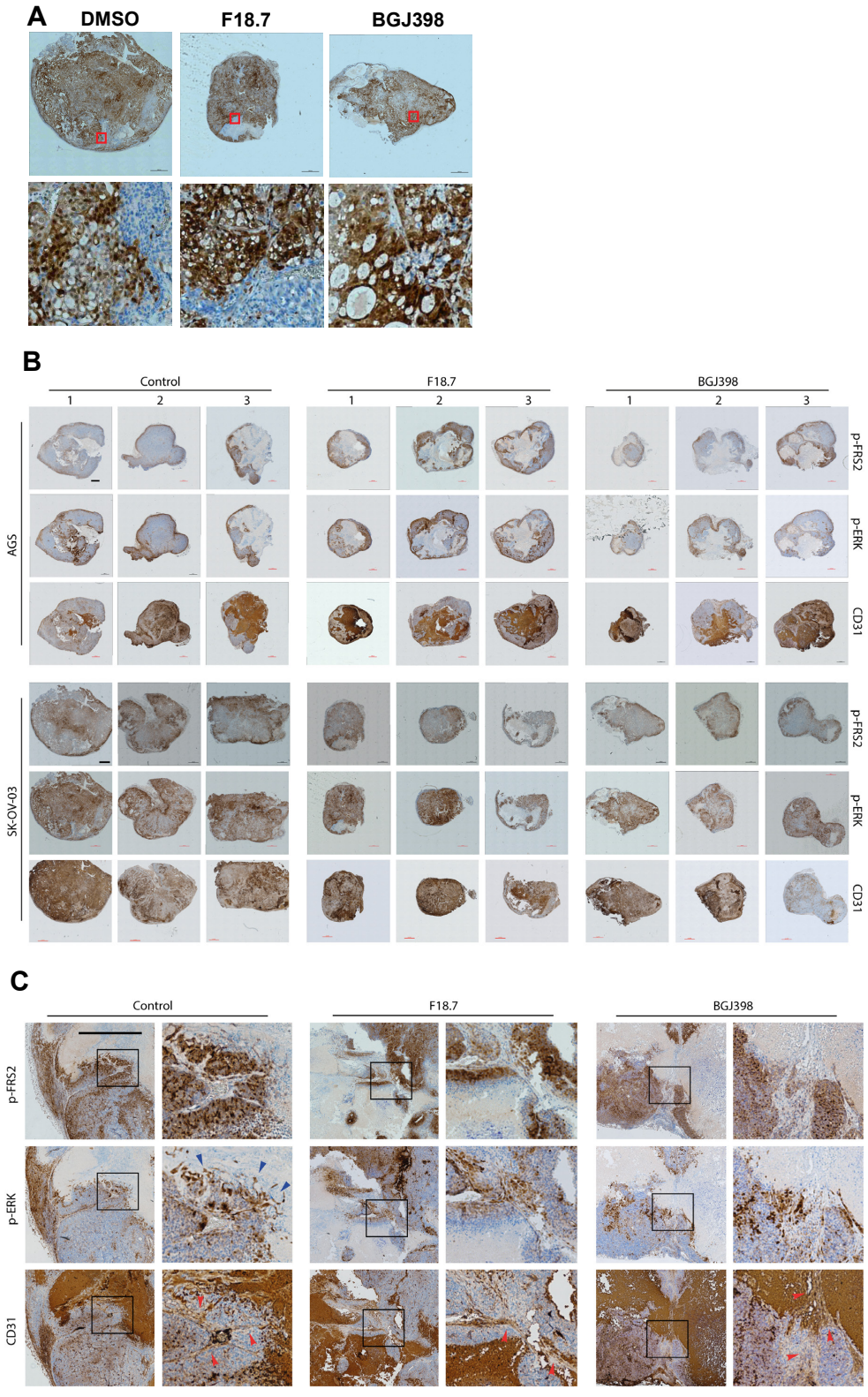
A
DMSO
F18.7
BGJ398
B
Control
F18.7
BGJ398
1
2
3
AGS
SK-OV-03
p-FRS2
p-ERK
CD31
C
Control
F18.7
BGJ398
p-FRS2
p-ERK
CD31

Figure S7

IHC analysis of SK-OV-3 and AGS cancer models. **A)** SK-OV-3 cancer section shown in Fig. 6E stained with anti-pERK antibody. Lower pictures are magnifications of red boxed areas. **B)** Overview of sections of three SK-OV-3 and AGS flank models and corresponding treatments. Sections were stained with anti-pERK antibodies. **C)** Areas in AGS tumors surrounding CD31-positive vessels. Red arrow heads indicate vessels, blue arrow heads pERK-positive invading cells. Right picture of each condition shows magnification of boxed area.